Bandstructure modulation for carbon nanotubes in a uniform electric field

James O'Keeffe
NASA Ames Research Center, Moffet Field, California 94035

Chengyu Wei, Kyeongjae Cho
Department of Mechanical Engineering, Stanford University, Stanford, California 94305-4040

(Received 2 July 2001; accepted for publication 31 October 2001)

A method to electronically modulate the energy gap and bandstructure of semiconducting carbon nanotubes is proposed. We investigate this bandstructure modulation mechanism using tight-binding and density functional theory (DFT). Results show that the energy gap of a semiconducting nanotube can be narrowed, when the tube is placed in an electric field perpendicular to the tube axis. In contrast, Metallic tubes were found to exhibit a screening behavior, whereby free charge redistributes about the tube circumference as a result of the external field. In this case, the bandstructure shows little perturbation in response to an applied electric field. © *2002 American Institute of Physics.* [DOI: 10.1063/1.1432441]

Carbon nanotubes possess several interesting physical and electronic properties. Semiconducting nanotubes have been grown up to several microns in length. In addition ohmic contacts to nanotubes have been demonstatated using Au and Pt electrodes.[1,2] Such properties have prompted research on single wall nanotubes (SWNT) as semiconducting channels in nanoscale field-effect transistors (FETs).[3,4] In a typical nanotube FET designs the tube acts as one of the MOS capacitor plates, as shown in Fig. 1(a). In response to a gate voltage, V_g larger than some threshold V_T, the fermi energy of the nanotube moves into the conduction or valence band. In cases where the gate oxide thickness is much greater than the tube diameter the nanotube reaches a uniform potential E_F at all points about the circumference. The charge on the tube is given by

$$Q_{\text{tube}} = \int_0^{E_F} eD(E) = C_g(V_g - V_T), \tag{1}$$

where $D(E)$ is the density of conduction or valence band states and C_g is the gate capacitance. In the ideal case this gives a conductance between the source and drain of ne^2/h, where n is the number of subbands which cross the fermi energy.

Here we have simulated the structure illustrated in Fig. 1(b). This structure has two main differences from the conventional nanotube MOS capacitor model. Firstly, instead of being one of the capacitor electrodes the nanotube is placed in the center of the dielectric gap. In this way the capacitor acts as a split-gate on the nanotube, with gate voltages of $\pm V_g/2$ respectively. Because of its position the fermi energy for the tube is maintained at 0 V in our simulations. The advantage of this approach is that no net charge must enter the nanotube to reach equilibrium, irrespective of the value of V_g. Second, the dielectric gap d is chosen to be similar to the nanotube diameter d_t. This results in a considerable portion of V_g appearing as a potential gradient at the atom locations about the nanotube circumference. We investigate changes in the band structure and conductance as a result of the potential gradient. This bandstructure modulation is similiar to that observed when the tube is mechanically deformed by flattening the tube cross section.[5] However, electronic control of the energy gap may be more viable for switching and circuit applications. The proposed energy gap modulation mechanism could allow hetrostructures to be created in uniform nanotubes, where a gating electric field is applied to several sections of the tube. Closely spaced hetrostructures also open the possibility for electrically controlled quantum confinement, in which the well shape could be dynamically varied. As the energy gap of the tube decreases there is an associated increase in tube conductance, which could be utilized in switching applications.

Following the formalism of Ref. 6 a nanotube can be described using a single π orbital hamiltonian as

$$H = \sum_i \epsilon_i c_i^* c_i + \sum_{i,j} t_{i,j} c_i^* c_j, \tag{2}$$

where ϵ_i is the unperturbed on-site potential and t_{ij} is the hopping parameter between lattice locations i and j. In the absence of defects, the unperturbed on-site potential ϵ_i is

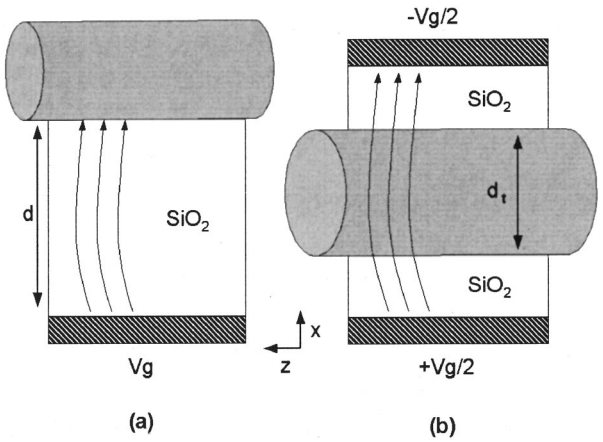

FIG. 1. (a) The nanotube acts as the semiconducting channel in a conventional nanotube MOSFET design. The tube acts as a capacitor plate and builds up a net surface charge Q_f. This is represented by electric field lines terminating at the nanotube surface. (b) A split-gate approach is used to create a potential gradient about the tube circumference. The nanotube is placed in the center of the dielectric and experiences no net charge.

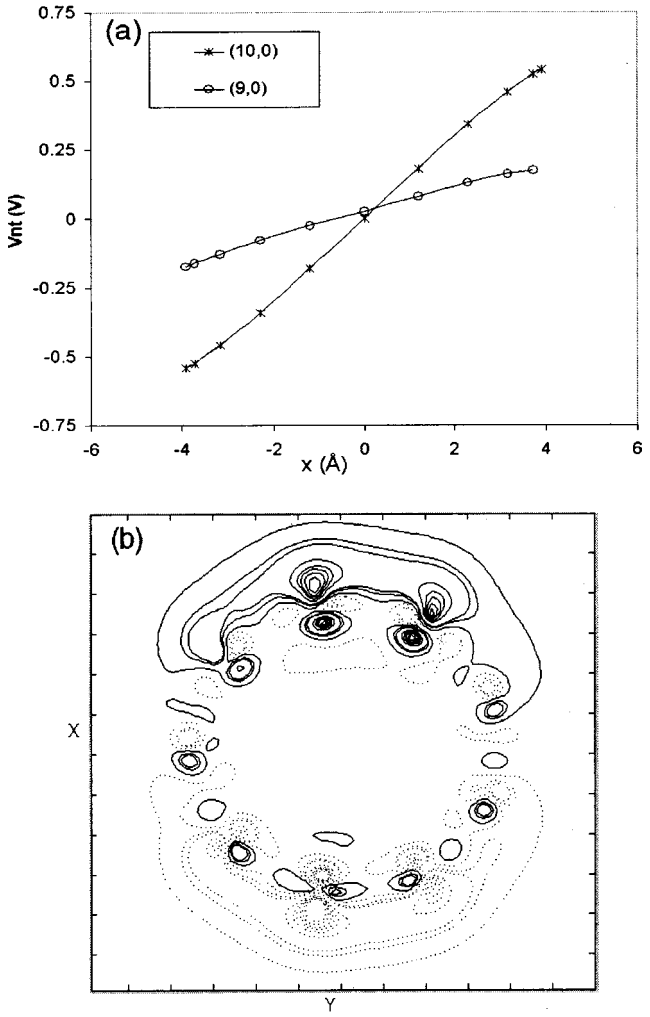

FIG. 2. (a) Equilibrium on-site atom potentials relative to the tube Fermi energy, shown as a function of distance from the tube axis. A field of 16.7 MeV/cm is applied perpendicular to the tube axis. In the case of a (10, 0) tube a peak atom potential of 0.59 eV appears about the tube circumference. A (9, 0) tube screens much of the electric field, which results in a smaller potential gradient. (b) Redistributed charge density for a (9, 0) tube. The net charge appears mainly in the π electron orbitals and acts to screen out the applied electric field. Positive charge is shown with solid contour lines and dotted contour lines represent negative charge. The plotted plane is normal to the tube axis and passes through one of the rings of carbon atoms.

zero and the hopping parameter $t_{ij}=-3.1$ eV.[7] c_i^*, c_i are the creation and annihilation operators at site i. In our case we use a 15 unit cell hamiltonian, for a zigzag $(n,0)$ nanotube, connected at each end to a semi-infinite $(n,0)$ lead. When a uniform electric field E_0 is applied across the tube cross-section, an external potential appears at the atom locations, given by $Vo_i=E_0x_i$, where x_i is the distance of each atom from the center axis of the tube. In response to the external potential, charges q_i appear at the atom locations. This charge is considered to have a screening effect on the external potential, in the same way that a metal cylinder would screen out all external electric fields. However, zigzag nanotubes do not exhibit ideal metallic behavior and a self-consistent solution method for the charge and equilibrium potential is employed. We consider a discrete distribution of point charges at the atom locations, which acts to reduce the net on-site potential Vnt according to

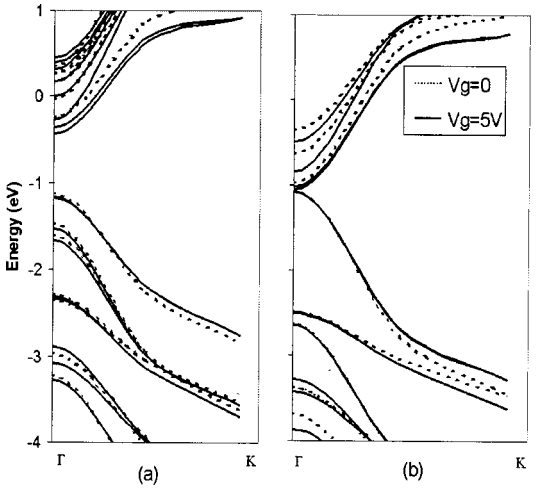

FIG. 3. Band structure modulation with applied gate voltage, $Vg=0$ V (dotted line), $Vg=5$ V (solid line). (a) A semiconducting (10,0) tube and (b) a metallic (9,0) tube.

$$Vnt_i=Vo_i+\sum_j^{N,n} q_j(4\pi\epsilon r_j)^{-1}. \tag{3}$$

The sum is conducted over the N unit cells in the Hamiltonian. Vnt was found to converge for $N>10$. Vnt_i at the center unit cell is used to update all equivalent locations on neighboring unit cells, as well as on the semi-infinite leads. The perturbed hamiltonain is given by

$$H=\sum_i [\epsilon_i+Vnt_i]c_i^*c_i+\sum_{i,j} t_{i,j}c_i^*c_j. \tag{4}$$

Finally, the net charge at the atom locations is given by

$$q_i=\frac{e}{\pi}\int_0^{E_F} \mathrm{Im}[G^r(E)_{i,i}]dE,$$

$$G^r(E)=[EI-H-\Sigma_L^r-\Sigma_R^r]^{-1}, \tag{5}$$

where G^r is the retarded system Green's function and $\Sigma_{L,R}^r$ are the self-energies of the left and right leads, respectively. We solve between Eqs. (4) and (6) to find a self-consistent solution. Equilibrium on-site potentials for a (9, 0) metallic nanotube and a (10, 0) semiconducting tube are shown in Fig. 2(a). $V_g=2$ V is applied across a 12 Å dielectric, resulting in a field of 16.7 MeV/cm. In the case of a metallic nanotube there is significant charge redistribution, which screens the applied potential. Figure 2(b) illustrates the net charge redistribution as a result of the gate voltage, calculated using the pseudopotential density functional theory approach described later. Most of the charge redistribution occurs between the π orbitals. In contrast, the (10, 0) tube supports a peak on-site potential of 0.59 eV. Results show that semiconducting tubes do not show any significant screening for $V_g<E_g(d/d_t)$, where d_t is the tube diameter. The reason for this is that the fermi energy at each atom location remains within the energy gap at low gate voltages.

The effect of a uniform electric field is also studied within the supercell approximation, using density functional theory (DFT). The simulation method used is described in Refs. 8,9.

Kohn–Sham single-electron wave functions are expanded over 17 900 plane waves. The supercell has dimen-

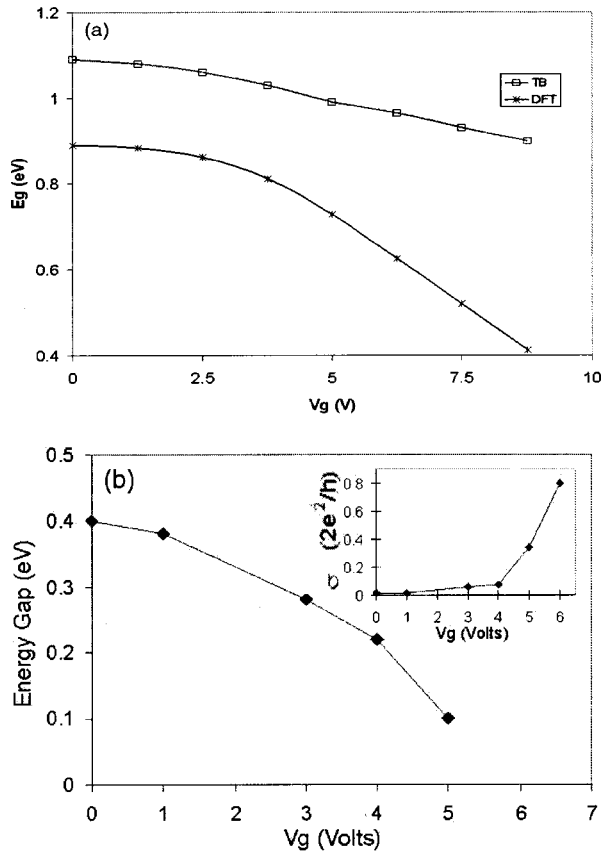

FIG. 4. (a) Energy gap reduction as a function of gate voltage for (10,0) tube. Density functional theory traditionally underestimates the size of the energy gap. (b) Energy gap reduction as a function of gate voltage for a (31,0) tube. The corresponding conductance increase is shown in the insert.

sions of $12\times12\times4.26$ Å^3. The separation of 4.26 Å in the direction of the tube axis results in an infinitely long tube. The Brillouin zone is sampled using three *k*-points along the tube axis. This is shown to agree closely with six *k*-point sampling in Ref. 10.

Figure 3(a) shows the perturbed band structure for a (10, 0) SWNT with a gate voltage $V_g=5$ V, calculated using the DFT analysis described above. The valence bands remain largely unchanged in the presence of a gate voltage, while the conduction bands move to lower energies. The energy gap is reduced from 0.89 eV to 0.73 V. In addition, the lowest conduction band, which exhibits a double degeneracy in the zero bias case, is split into two separate energy levels, separated by 0.11 eV. This perturbation in the energy eigenvalues and band gap is caused by the nonuniform potential gradient about the tube circumference. In contrast, Fig. 3(b) illustrates that the HOMO-LUMO bandstructure of a (9,0) tube remains unchanged close to the brillouin zone center.

Energy gap variation with gate voltage is illustrated in Fig. 4(a). The tight-binding analysis predicts a 1.08 eV energy gap for a (10,0) SWNT under zero gate bias conditions. Other experimental and theoretical work agrees closely with this value.[11] The DFT results underestimate the zero bias energy gap by almost 20%. This error is common in DFT simulations of semiconductors and several correction factors have been proposed.[12] Both the DFT and tight-binding results show a linear reduction in energy gap size after some threshold gate voltage V_{th}.

For the purposes of this work we simulated small diameter (10,0) and (9,0) SWNTs. A large electric field >20 MeV/cm was required to produce significant on-site energy variation across the small tube diameter. While these tube sizes are practical for DFT simulation the associated high fields make experimental implementation difficult. To address this issue we simulated (31,0) zigzag tubes, in which the potential gradient was supported across a larger 2.42 nm diameter. The variation of tube conductance and energy gap size are illustrated in Fig. 4(b). It is found that the energy gap reduces from 0.4 eV to 0.2 eV for a uniform electric field of 6.7 Mev/cm.

In conclusion, we present a method to modulate the energy gap of semiconducting carbon nanotubes, by establishing a potential gradient about the tube circumference. Metallic tubes were found to exhibit lower equilibrium potential gradients, which is consistent with charge screening behavior at a metal surface.

We would like to thank Dr. N. Mingo and Dr. M. Anantram (NASA Ames Research Center) for useful discussions

[1] A. Bachtold, M. Henny, C. Terrier, C. Srtunk, C. Schronenberger, J.-P. Salvetat, J.-M. Bonard, and L. Forro, Appl. Phys. Lett. **73**, 274 (1998).
[2] S. J. Tans, M. H. Devoret, H. Dai, A. Thess, R. E. Smalley, L. J. Geerligs, and C. Dekker, Nature (London) **386**, 474 (1997).
[3] S. J. Tans, A. R. M. Verschueren, and C. Dekker, Nature (London) **393**, 49 (1998).
[4] R. Martel, T. Schmidt, H. R. Shea, T. Hertel, and Ph. Avouris, Appl. Phys. Lett. **73**, 2447 (1998).
[5] C. J. Park, Y. H. Kim, and K. J. Chang, Phys. Rev. B **60**, 10656 (1999).
[6] M. P. Anantram, and T. R. Govindan, Phys. Rev. B **58**, 4882 (1998).
[7] J.-C. Charlier, T. W. Ebbesen, and Ph. Lambin, Phys. Rev. B **53**, 11108 (1996).
[8] M. C. Payne, M. P. Teter, D. C. Allan, T. A. Arias, and J. D. Joannopoulos, Rev. Mod. Phys. **64**, 1045 (1992).
[9] C. Wei, "Structure and vibrations of vicinal surfaces and field-induced structure modification: An ab initio study" Chapter 4, Ph. d. Thesis (2000).
[10] S. Peng and K. Cho, Nanotechnology **11**, (2000).
[11] Riichiro Saito, G. Dresselhaus, and M. S. Dresselhaus, J. Appl. Phys. **73**, 494 (1993).
[12] L. J. Sham and M. Schluter, Phys. Rev. Lett. **51**, 1888 (1983).